Evaluation of Integrated Tuning Elements with SIS Devices

M. M. T. M. Dierichs, C. E. Honingh, R. A. Panhuyzen, B. J. Feenstra, A. Skalare, J. J. Wijnbergen, H. v.d. Stadt, and Th. de Graauw

Abstract—**The resonances of integrated tuning stubs in combination with SIS detectors are measured and calculated. The predicted resonances are compared with measurements of stubs integrated with $Nb/Al_2O_3/Nb$ junctions in a log-periodic antenna. Stubs of different lengths have been investigated on different substrates (on 200 μm thick quartz and on a 7 μm thick silicon membrane) and the results show a fairly good agreement with the model calculations. Quartz substrates showed resonances up to 640 GHz, while for silicon membranes stub resonances reach up to as 480 GHz. An observed resonance at 560 GHz is probably a substrate effect from the membrane. The gap frequency for all the samples is 670 GHz and no resonances are detected above this frequency. Up to the maximum detected frequency dispersion is found to be negligible.**

I. Introduction

SIS MIXERS with $Nb/Al_2O_3/Nb$ junctions are very sensitive submm detectors. Recent progress in SIS mixer development is due to the ability to manufacture smaller junctions down to sub-micron dimension [1], [2]. Instead of continuing to put more effort into the fabrication of smaller junctions and thus reducing the junction capacitance, it is also possible to implement integrated tuning elements, which are fairly easy to fabricate and result in a high sensitivity and broad bandwith. It has been shown that junctions with integrated tuning used in submm-wave mixers give good results [3], [4].

The first published stub measurements used self-pumped steps in the I-V characteristic to measure the resonance of the stub [5]. A more accurate and complete evaluation can be performed with a Fourier Transform Spectrometer (FTS) as shown by Hu *et al* [6].

For our work we have designed stubs for 100 GHz and 350 GHz. The first type has multiple resonances to estimate dispersion in the niobium stubs. These antennas are made on 200 μm thick quartz substrates and on 7 μm silicon membranes. From the second type the material parameters are determined.

In this paper we describe first the theoretical background in Sec. II, the fabrication results are presented in Sec. III, the experimental details are described in Sec. IV, the comparison between theory and experiment is discussed in Sec. V, and the conclusion will be drawn in Sec. VI.

II. Model Calculation

To tune out the geometric capacitance of the junction an inductive tuning element (stub) is required. Two junctions in series, placed in the center of a log-periodic antenna, with a stub for each junction is used. The total arrangement is modelled with the circuit shown in Fig. 1. For completeness the connecting strip between the two junctions is included as an inductor L_{leads}. In practice this inductance can be neglected in evaluating the frequency response.

Using integrated tuning, the junction impedance can not simply be described as a pure resistor with a parallel capacitor. Instead, it must be described as a capacitor in parallel with a complex admittance with a conductive part (G_Q) and a susceptive part (B_Q). Since the experiment works in the small signal limit and the Josephson effect is suppressed by a magnetic field, the junction admittance can be described as follows [7], [8].

$$G_Q = \frac{e}{2\cdot\hbar\cdot\omega}\cdot\left[I_{\text{dc}}\left(V_0+\frac{\hbar\cdot\omega}{e}\right) - I_{\text{dc}}\left(V_0-\frac{\hbar\cdot\omega}{e}\right)\right] \quad (1)$$

$$B_Q = \frac{e}{2\cdot\hbar\cdot\omega}\cdot\left[I_{kk}\left(V_0+\frac{\hbar\cdot\omega}{e}\right) - 2\cdot I_{kk}(V_0) + I_{kk}\left(V_0-\frac{\hbar\cdot\omega}{e}\right)\right] \quad (2)$$

These equations show that the resonant frequency depends on the bias voltage and the photon-energy. In these equations is $\hbar\omega/e$ the energy of the photon step, V_0 is the bias voltage, and

$$I_{kk} = P\int_{-\infty}^{\infty}\frac{dV'}{\Pi}\cdot\frac{I_{\text{dc}}(V')-\dfrac{V'}{R_n}}{V'-V} \quad (3)$$

where I_{kk} is the Kramers-Kronig transform, which can be calculated from the dc-IV curve. The inductance per unit length of the stub can be calculated as follows [9].

$$L_s = \frac{\mu_0}{k\cdot w}\cdot\left[t_d+\frac{\lambda}{\tanh\left(\dfrac{t_1}{\lambda}\right)}+\frac{\lambda}{\tanh\left(\dfrac{t_2}{\lambda}\right)}\right] \quad (4)$$

Manuscript received June 2, 1992.
M. M. T. M. Dierichs and B. J. Feenstra are with the Department of Applied Physics and Materials Science Centre, University of Groningen, Nijenborgh 4, 9747 AG Groningen, The Netherlands.
C. E. Honingh, R. A. Panhuyzen, A. Skalare, J. J. Wijnbergen, H. v.d. Stadt, and Th. de Graauw are with the Space Research Organization of the Netherlands, Groningen, Landleven 12, 9747 AD Groningen, The Netherlands.
IEEE Log Number 9206311.

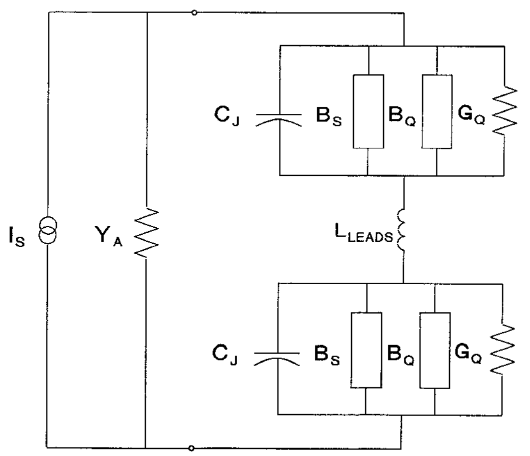

Fig. 1. Electrical equivalent of two junctions in series with integrated tuning elements.

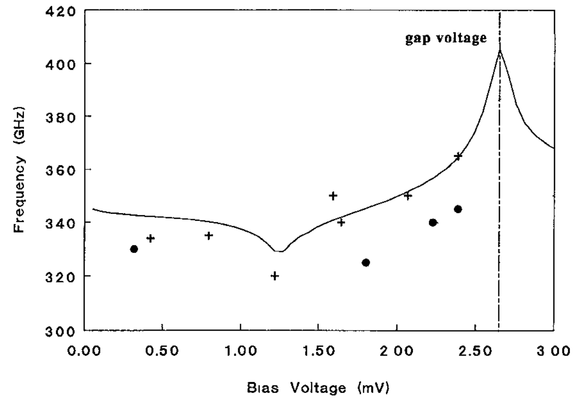

Fig. 2. Calculated (lines) and measured (marks) resonant frequencies as a function of bias voltage for two different junction batches with two different stub lengths (crosses and solide line; length is 119 μm, circles and dashed line; length is 127 μm).

where w is the width of the stub, k is the fringing factor [10], t_1, t_2 and t_d are the thicknesses of the ground plane, the stub, and the dielectric layer respectively, and λ is the penetration depth of the niobium layers. The capacitance per unit length of the stub is given by

$$C_s = K \cdot \epsilon_{\text{eff}} \cdot \epsilon_0 \cdot \frac{w}{t_d} \tag{5}$$

Knowing the capacitance and the inductance of the stub, the impedance Z_0 and the phase velocity v_0 follow from the definitions:

$$Z_0 = \sqrt{\frac{L_s}{C_s}} \tag{6}$$

$$v_0 = \frac{1}{\sqrt{L_s \cdot C_s}} \tag{7}$$

The RF coupling coefficient C_{RF} defined as the fraction of the available power dissipated in the junction is given by

$$C_{\text{RF}} = 1 - \left| \frac{Y_A - Y_J^*}{Y_A + Y_J} \right|^2 \tag{8}$$

where $Y_A = 1/R_A$ is the simplified admittance of the antenna (1/60 Ω)^6, and Y_J is the admittance of the right hand side of Fig. 2.

III. Fabrication of Devices

The detector is positioned in the center of a broad-banded log-periodic antenna. We use 2 junctions in series of each 1 μm^2 and a current density of 12000 A/cm^2. On top of the junctions the wiring layer (600 nm niobium) is defined with a stub for each junction (Fig. 1). The dielectric layer between the ground plane (antenna) and the stub is 250 nm thick sputtered SiO_2. The junctions are fabricated with the Selective Niobium Over-Etch Process (SNOEP) [11].

Antennas are fabricated on 200 μm thick quartz substrates and on 7 μm thick silicon membranes. The membranes have been etched in ethlyenediamine-pryocatechol-water (EPW) [12]. The junctions on the membranes were fabricated after the etching of the membranes and are of the same quality as the junctions fabricated on the quartz substrate. With the obtained thickness, the membrane is transparent which simplifies the alignment of the antenna on the membrane.

IV. Measurement Set-Up

For measuring the response of the detector, we use a FTS with a Hg arc lamp as source [13]. The operating frequency range is determined by a 50 μm thick kapton film beam-splitter. The mechanical traveling distance was 50 mm resulting in a resolution of 4 GHz.

The antenna is mounted in a liquid helium dewar with dc-bias connections. All antennas fabricated on a quartz substrate are glued to a quartz hyper-hemispherical lens. The lens optimizes the optical coupling and results in a better sensitivity. The measurements performed with the log-periodic antenna on a thin membrane are without lens, resulting in a lower signal and a higher noise level. The substrate is not glued to the lens to prevent the occurrance of standing waves between the lens and the membrane.

V. Results

A. Short Stubs on 200 μm Quartz Substrates.

Antennas with stub lengths around 120 μm are investigated to determine the specific capacitance of the junction and the penetration depth of the niobium layers. Resonant frequencies are measured from two different batches with two different stub lengths. The resonant frequency is depending on the bias voltage due to the behaviour of the quantum impedance (1) and (2). The maximum in the resonant frequency is due to the maximum in the Kramers-Kronig transform. Calculated and measured results are shown in Fig. 2. Best agreement between theory and experiment is obtained with the assumption of a specific capacitance of 55 ± 5 fF/μm^2 and a penetration depth of 100 $\pm$ 5 nm. These values are further used in the calculations of the long stubs. Differences between calculations and measurements are due to the noise in the spectrogram which complicates the determination of the resonant frequencies. No multiple resonance is observed above 670 GHz.

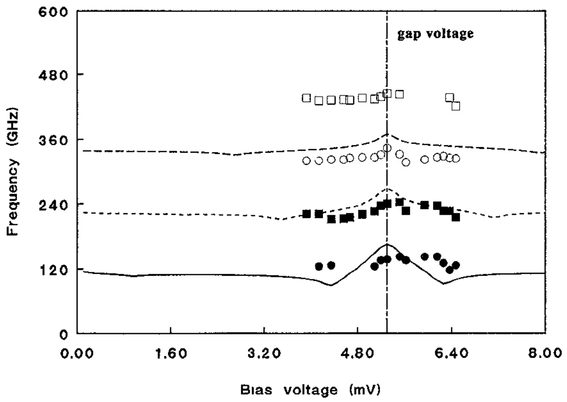

Fig. 3. Calculated and measured resonance frequencies for an antenna with a 527 μm long stub on a quartz substrate as a function of bias voltage.

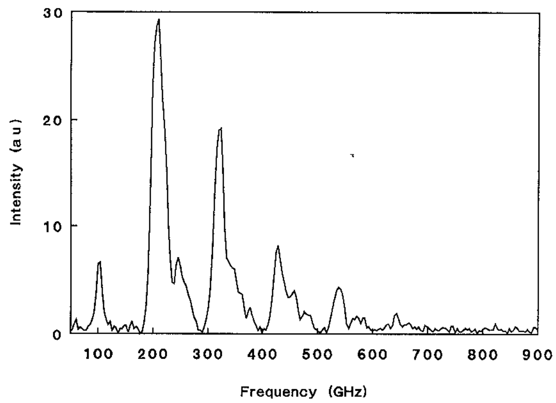

Fig. 4. Frequency response of a 527 μm long stub.

B. Long Stubs on 200 µm Quartz Substrates

Next, the resonances of a 527 μm long stub on a quartz substrate are measured. The results of the measurements at different bias voltages are plotted in Fig. 3 and are compared with model calculations. The observed resonances agree fairly well with the model both below as well as above the gap voltage. Only the first four resonances are displayed because they can always be identified from the noise. The frequency response is shown in Fig. 4. Stub resonances up to 640 GHz are observed, while no antenna resonances are visible. We observe some dispersion in the resonances, which is probably due to losses in the niobium stub.

C. Long Stubs on 7 µm Silicon Membranes

The resonances of a 527 μ m long stub on a 7 μm thick silicon membrane are measured. The resolution (8 GHz) is lower because the scan length was decreased. We observe stub resonances at 110, 200, and 325 GHz. Incidentally resonances at 165, 310, and 540 GHz occur which are probably substrate resonances. The highest stub resonance appears to be at 450 GHz which is lower than the measurements on quartz. This is due to the decreased signal level. The lowest three resonances are compared with the model calculations in Fig. 5. Also here the measurements agree fairly well with the model. The spread in data is due to the lower resolution and the increased noise level.

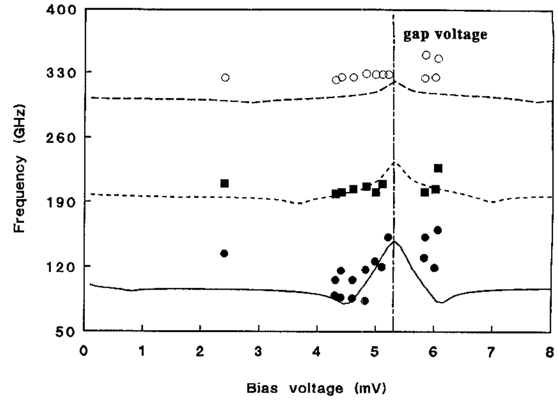

Fig. 5. Calculated and measured resonance frequencies for an antenna on a silicon membrane with a 527 μm long stub as a function of bias voltage.

VI. Conclusions

The model calculations and the experimental results for the short stubs lead to a penetration depth of 100 nm and a specific capacitance of 55 fF/μm^2. This is independent of the measured batch. For long stubs the model predicts the resonances fairly well. The measured frequency shift at the higher resonances is probably due to dispersion. Both below and above the gap voltage the resonances agree fairly well with the model. Resonances up to 640 GHz are observed. For antennas fabricated on 7 μm thick silicon membranes resonances only up to 480 GHz are observed due to the bad beam coupling. Also possible substrate resonances are measured. No resonances above 670 GHz are observed, which is the gap frequencies of niobium.

Acknowledgment

We thank T. M. Klapwijk for his stimulating discussions, H. G. Golstein and G. de Groot for their help with the Michelson interferometer, M. J. de Boer for etching the membranes, G. de Lange for his support with the model calculation and H. H. A. Schaeffer for the mechanical support. This work supported by the Stichting Technische Wetenschappen (STW) and the Stichting voor Fundamenteel Onderzoek der Materie (FOM), which are part of the Nederlandse Organisatie voor Wetenschappelijk Onderzoek (NWO). We acknowledge the financial support of the European Space Research (ESA) through contract 7898/88NL/PB(SC).

References

[1] W. R. McGrath, H. H. S. Javadi, S. R. Cypher, B. Bumble, B. D. Hunt, and H. G. LeDuc, "Low noise 205 GHz SIS mixers using high current density Nb and NbN tunnel junctions," *Proc. Second Int. Symp. on Space Terahertz Technology,* 1991, pp. 423–438.

[2] J. W. Kooi, M. Chan, T. G. Phillips, B. Bumble, and H. G. LeDuc. "A low noise 230 GHz heterodyne receiver employing .25 μm^2 area Nb/AlOx/Nb tunnel junctions," *IEEE Trans Microwave Theory Tech.*, vol. 40, no. 5, pp. 812–815, 1992.

[3] A. W. Lichtenberger, D. M. Lea, A. C. Hicks, J. D. Prince, R. Densing, D. Peterson, and B. S. Deaver, "Nb/Al-Al_2O_3/Nb junctions with inductive tuning elements for a very low noise 205–250 GHz heterodyne receiver," *IEEE Trans. Microwave Theory Tech.*, vol. 40, no. 5, pp. 816–819, 1992.

[4] J. Zmuidzinas, and H. G. LeDuc, "Quasi-optical slot antenna SIS mixers," *Proc. Second Int. Symp. on Space Terahertz Technology*, 1991, pp. 481–490.

[5] A. V. Räisänen, W. R. McGrath, P. L. Richards, and F. L. Lloyd, "Broadband RF match to a millimeter-wave SIS quasi quasi-particle mixer," *IEEE Trans Microwave Theory Tech.,* vol. MTT-33, pp. 1495–1499, 1985.
[6] Q. Hu, C. A. Mears, P. L. Richards, and F. L. Lloyd, "Measurement of integrated tuning elements for SIS mixers with a Fourier transform spectrometer," *Int. J. Infrared and MM Waves,* vol. 9, pp. 303–320, 1988.
[7] J. R. Tucker, and M. J. Feldman, "Quantum detection at millimeter wavelength," *Rev. Mod. Phys.*, vol. 57, pp. 1055–1113, 1985.
[8] Q. Hu, C. A. Mears, P. L. Richards,. and F. L. Lloyd, "Quantum susceptance and its effects on the high-frequency response of superconducting tunnel junctions," *Phys. Rev. B,* vol. 42, pp. 10 250–10 263, 1990.
[9] J. C. Swihart, "Field solution for a thin-film superconducting strip transmission line," *J. Appl. Phys.*, vol. 32, pp. 461–469, 1961.
[10] W. H. Chang, "The inductance of a superconducting strip transmission line," *J. Appl. Phys.,* vol. 50, pp. 8129–8134, 1979.
[11] M. M. T. M. Dierichs, R. A. Panhuyzen, C. E. Honingh, M. J. de Boer, and T. M. Klapwijk, "Sub-micron niobium junctions for submillimeter-wave mixers using optical lithography," *Appl. Phys. Lett.*, vol. 62, pp. 774–777, 1993.
[12] K. E. Petersen, *Proc. IEEE,* vol. 70, p. 420, 1982.
[13] P. L. Richards, in *Spectroscopic Technique for Far Infrared Submillimeter and Milimeter Waves.* Amsterdam: North-Holland, 1967.

M. M. T. M. Dierichs, photograph and biography not available at the time of publication.

C. E. Honingh, photograph and biography not available at the time of publication.

R. A. Panhuyzen, photograph and biography not available at the time of publication.

B. J. Feenstra, photograph and biography not available at the time of publication.

A. Skalare, photograph and biography not available at the time of publication.

J. J. Wijnbergen, photograph and biography not available at the time of publication.

H. v.d. Stadt, photograph and biography not available at the time of publication.

Th. de Graauw, photograph and biography not available at the time of publication.